

1 Soil Moisture and Hydrology Projections of the Permafrost 2 Region: A Model Intercomparison

3 Christian G. Andresen^{1,2}, David M. Lawrence³, Cathy J. Wilson¹, A. David McGuire⁴, Charles
4 Koven⁵, Kevin Schaefer⁶, Elchin Jafarov^{6,1}, Shushi Peng⁷, Xiaodong Chen⁸, Isabelle
5 Gouttevin^{9,10}, Eleanor Burke¹¹, Sarah Chadburn¹², Duoying Ji¹³, Guangsheng Chen¹⁴, Daniel
6 Hayes¹⁵, Wenxin Zhang^{16,17}

7
8 ¹Earth and Environmental Science Division, Los Alamos National Laboratory, Los Alamos, New Mexico, USA

9 ²Geography Department, University of Wisconsin Madison, Madison, Wisconsin, USA

10 ³National Center for Atmospheric Research, Boulder, Colorado, USA

11 ⁴Institute of Arctic Biology, University of Alaska Fairbanks, Fairbanks, Alaska, USA

12 ⁵Climate and Ecosystem Sciences Division, Lawrence Berkeley National Lab, Berkeley, CA, USA

13 ⁶Institute of Arctic Alpine Research, University of Colorado Boulder, Boulder, Colorado, USA

14 ⁷UJF–Grenoble 1/CNRS, Laboratoire de Glaciologie et Géophysique de l'Environnement (LGGE), Grenoble, France

15 ⁸Department of Civil and Environmental Engineering, University of Washington, Seattle, Washington, USA

16 ⁹IRSTEA-HHLY, Lyon, France.

17 ¹⁰IRSTEA-ETNA, Grenoble, France.

18 ¹¹Met Office Hadley Centre, UK

19 ¹²School of Earth and Environment, University of Leeds, UK

20 ¹³College of Global Change and Earth System Science, Beijing Normal University, China

21 ¹⁴Environmental Sciences Division, Oak Ridge National Laboratory, Oak Ridge, Tennessee, USA

22 ¹⁵ School of Forest Resources, University of Maine, Maine, USA

23 ¹⁶ Department of Physical Geography and Ecosystem Science, Lund University, Lund, Sweden

24 ¹⁷Center for Permafrost (CENPERM), Department of Geosciences and Natural Resource Management, University of
25 Copenhagen, Denmark

26
27 *Correspondence to:* Christian G. Andresen (candresen@wisc.edu)

28
29 **Abstract.** This study investigates and compares soil moisture and hydrology projections of broadly-used
30 land models with permafrost processes and highlights the causes and impacts of permafrost zone soil
31 moisture projections. Climate models project warmer temperatures and increases in precipitation (P)
32 which will intensify evapotranspiration (ET) and runoff in land models. However, this study shows that
33 most models project a long-term drying of the surface soil (0-20cm) for the permafrost region despite
34 increases in the net air-surface water flux (P-ET). Drying is generally explained by infiltration of moisture
35 to deeper soil layers as the active layer deepens or permafrost thaws completely. Although most models
36 agree on drying, the projections vary strongly in magnitude and spatial pattern. Land-models tend to agree
37 with decadal runoff trends but underestimate runoff volume when compared to gauge data across the
38 major Arctic river basins, potentially indicating model structural limitations. Coordinated efforts to
39 address the ongoing challenges presented in this study will help reduce uncertainty in our capability to
40 predict the future Arctic hydrological state and associated land-atmosphere biogeochemical processes
41 across spatial and temporal scales.

42 43 1. Introduction

44
45 Hydrology plays a fundamental role in permafrost landscapes by modulating complex interactions among
46 biogeochemical cycling (Frey and McClelland, 2009; Newman et al., 2015; Throckmorton et al., 2015),
47 geomorphology (Grosse et al., 2013; Kanevskiy et al., 2017; Lara et al., 2015; Liljedahl et al., 2016) and
48 ecosystem structure and function (Andresen et al., 2017; Avis et al., 2011; Oberbauer et al., 2007).
49 Permafrost has a strong influence on hydrology by controlling surface and sub-surface distribution,

50 storage, drainage and routing of water. Permafrost prevents vertical water flow which often leads to
51 saturated soil conditions in continuous permafrost while confining subsurface flow through perennially-
52 unfrozen zones (a.k.a. taliks) in discontinuous permafrost (Jafarov et al., 2018; Walvoord and Kurylyk,
53 2016). However, with the observed (Streletskiy et al., 2008) and predicted (Slater and Lawrence, 2013)
54 thawing of permafrost, there is a large uncertainty in the future hydrological state of permafrost
55 landscapes and in the associated responses such as the permafrost carbon-climate feedback.

56 The timing and magnitude of the permafrost carbon-climate feedback is, in part, governed by changes in
57 surface hydrology, through the regulation by soil moisture of the form of carbon emissions from thawing
58 labile soils and microbial decomposition as either CO₂ or CH₄ (Koven et al., 2015; Schädel et al., 2016;
59 Schaefer et al., 2011). The impact of soil moisture changes on the permafrost-carbon feedback could be
60 significant. Lawrence et al. (2015) found that the impact of the soil drying projected in simulations with
61 the Community Land Model decreased the overall Global Warming Potential of the permafrost carbon-
62 climate feedback by 50%. This decrease was attributed to a much slower increase in CH₄ emissions if
63 surface soils dry, which is partially compensated for by a stronger increase in CO₂ emissions under drier
64 soil conditions.

65 Earth System Models project an intensification of the hydrological cycle characterized by a general
66 increase in the magnitude of water fluxes (e.g. precipitation, evapotranspiration and runoff) in northern
67 latitudes (Rawlins et al., 2010; Swenson et al., 2012). In addition, intensification of the hydrological cycle
68 is likely to modify the spatial and temporal patterns of water in the landscape. However, the spatial
69 variability, timing, and reasons for future changes in hydrology in terrestrial landscapes in the Arctic are
70 unclear and variability in projections of these features by current terrestrial hydrology applied in the
71 Arctic have not been well documented. Therefore, there is an urgent need to assess and better understand
72 hydrology simulations in land models and how differences in process representation affect projections of
73 permafrost landscapes.

74 Upgrades in permafrost representation such as freeze and thaw processes in the land component of Earth
75 System Models have improved understanding of the evolution of hydrology in high northern latitudes.
76 Particularly, soil thermal dynamics and active layer hydrology upgrades include the effects of unfrozen
77 water on phase change, insulation by snow (Peng et al., 2015), organic soils (Jafarov, E. and Schaefer,
78 2016; Lawrence et al., 2008) and cold region hydrology (Swenson et al., 2012). Nonetheless, large
79 discrepancies in projections remain as the current generation of models substantially differ in soil thermal
80 dynamics (e.g. Peng *et al* 2015, Wang *et al* 2016). In particular, variability among current models’
81 simulations of the impact of permafrost thaw on soil water and hydrological states is not well
82 documented. Therefore, in this study we analyze the output of a collection of widely-used “permafrost-
83 enabled” land models. These models participated in the Permafrost Carbon Network Model
84 Intercomparison Project (PCN-MIP) (McGuire et al., 2018, 2016) and contained the state-of-the art
85 representations of soil thermal dynamics in high latitudes at that time. In particular, we assess how
86 changes in active layer thickness and permafrost thaw influence near-surface soil moisture and hydrology
87 projections under climate change. In addition, we provide comments on the main gaps and challenges in
88 permafrost hydrology simulations and highlight the potential implications for the permafrost carbon-
89 climate feedback.

90
91
92
93

94 2. Methods

95

96 2.1 Models and Simulation Protocol

97

98 This study assesses a collection of terrestrial simulations from models that participated in the PCN-MIP
99 (McGuire et al., 2018, 2016) (Table 1). The analysis presented here is unique as it focuses on the
100 hydrological component of these models. Table 2 describes the main hydrological characteristics for each
101 model. Additional details on participating models regarding soil thermal properties, snow, soil carbon and
102 forcing trends can be found in previous PCN-MIP studies (e.g. McGuire *et al* 2016, Koven *et al* 2015,
103 Wang *et al* 2016, Peng *et al* 2015). It is important to note that the versions of the models presented in this
104 study are from McGuire *et al* (2016, 2018) and some additional improvements to individual models may
105 have been made since then.

106 The simulation protocol is described in detail in *McGuire et al.*, (2016, 2018). In brief, models'
107 simulations were conducted from 1960 to 2299, partitioned by historic (1960-2009) and future
108 simulations (2010-2299), where future simulations were forced with a common projected climate derived
109 from a fully coupled climate model simulation (CCSM4) (Gent et al., 2011). Historic atmospheric forcing
110 datasets (Table 1) (e.g. climate, atmospheric CO₂, N deposition, disturbance, etc.) and spin-up time were
111 specific to each modeling group. The horizontal resolution (0.5° – 1.25°) and soil hydrological column
112 configurations (depths ranging from 2 to 47m and 3 to 30 soil layers) also vary across models (Figure 1).
113 We focus on results from simulations forced with climate and CO₂ from the Representative Concentration
114 Pathway (RCP) 8.5 scenario, which represents unmitigated, “business as usual” emissions of greenhouse
115 gases. Future simulations were calculated from monthly CCSM4 (Gent et al., 2011) climate anomalies for
116 the Representative Concentration Pathway (RCP 8.5, 2006-2100) and the Extension Concentration
117 Pathway (ECP 8.5, 2101-2299) scenarios, relative to repeating (1996-2005) forcing atmospheric datasets
118 from the different modeling groups (Table 1).

119 The choice of the PCN model intercomparison was to use output from a single Earth System model
120 climate projection was motivated by a desire to keep the experimental design simple and computationally
121 tractable. Clearly, using just one climate projection does not allow us to explore the impact of the broad
122 range of potential climate outcomes that are seen across the CMIP5 models. Instead, the PCN suite of
123 simulations allows for a relatively controlled analysis of the spread of model responses to a single
124 representative climate trajectory. The selection of CCSM4 as the climate projection model was motivated
125 partly by convenience and also because it was one of the only models that had been run out to the year
126 2300 at the time of the PCN experiments. Further, as noted in McGuire et al. (2018), CCSM4 late 20th
127 century climate biases in the Arctic were among the lowest across the CMIP5 model archive. It should be
128 noted that the use of a single climate projection means that the results presented here should be viewed as
129 indicative of just one possible permafrost hydrologic trajectory. As we will show, even under this single
130 climate trajectory, the range of hydrologic responses in the models are broad, indicating high structural
131 uncertainty across models with respect to this particular aspect of the Arctic system response to global
132 climate change.

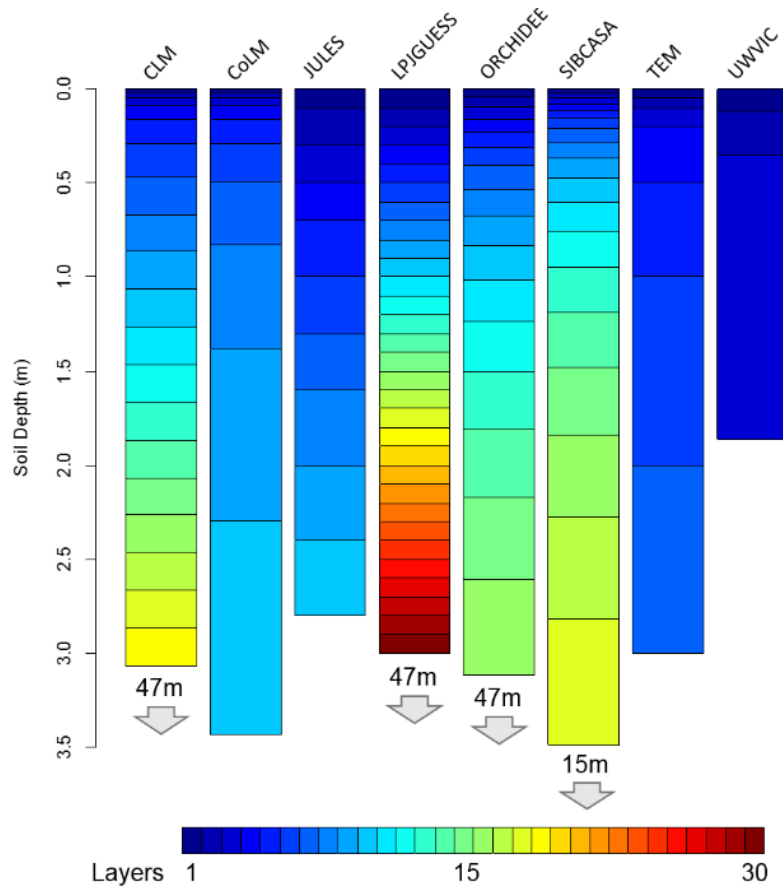
133 2.2 Permafrost and Hydrology Variables Analyzed

134

135 Our analysis focused on the permafrost regions in the Northern Hemisphere north of 45°N . This
136 qualitative hydrology comparison was based on the full permafrost domain for each model rather than a
137 common subset among models in order to fully portray the overall changes in permafrost hydrology for
138 participating models. For each model, we define a grid cell as containing near-surface permafrost if the
139 annual monthly maximum active layer thickness (ALT) is at or less than the 3m depth layer depending on
140 the model soil configuration (Figure 1) (McGuire et al., 2016; Slater and Lawrence, 2013). Participating
141 models represent frozen soil for layers with temperature of $<273.15^{\circ}\text{K}$, acting as an impermeable layer for
142 liquid water. We assessed how permafrost changes affect near-surface soil moisture, defined here as the
143 soil water content (kg/m^3) of the 0-20 cm soil layer. We focused on the top 20 cm of the soil column due
144 to its relevance to near-surface biogeochemical processes. We added the weighted fractions for each
145 depth interval to calculate near-surface soil moisture (0-20cm) to account for the differences in the
146 vertical resolution of the soil grid cells among models (Figure 1). To better understand the causes and
147 consequences of changes in soil moisture, we examined several principal hydrology variables including
148 evapotranspiration (ET), runoff (R; surface and sub-surface) and precipitation (P; snow and rain).
149 Representation of ET, R and soil hydrology varies across participating models and are summarized in
150 table 2.

151 We compared model simulations with long-term (1970-1999) mean monthly discharge data from Dai *et al*
152 2009. We computed model total annual discharge (sum of surface and subsurface runoff) for the main
153 river basins in the permafrost region of North America (Mackenzie, Yukon) and Russia (Yenisei, Lena).
154 In particular, we compared (i) annual runoff anomalies, (ii) correlation coefficients and (iii) distributions
155 of annual discharge between gauge data and models' simulations for the 30-year period of 1970-1999.
156 Gauge stations from major permafrost river basins used for simulation comparison include (i) Arctic Red,
157 Canada (67.46°N , 133.74°W) for Mackenzie River, (ii) Pilot Station, Alaska (61.93°N 162.88°W) for
158 Yukon River, (iii) Igarka, Russia (67.43°N , 86.48°E) for Yenisey River and (iv) Kusur, Russia (70.68°N ,
159 127.39°E) for Lena River.

160



161
162
163
164
165
166
167
168

Figure 1. Soil hydrologically-active column configuration for each participating model. Numbers and arrows indicate full soil configuration of non-hydrologically active bedrock layers. Colors represent the number of layers.

Table 1. Models description and driving datasets.

Model	Full Name	Climate Forcing Dataset	Model Reference	Short-Wave radiation ^a	Long-Wave Radiation ^a	Vapor Pressure ^a
CLM 4.5	Community Land Model v4.5	CRUNCEP4 ^b	Oleson <i>et al</i> (2013)	Yes	Yes ^c	Yes
CoLM	Common Land Model	Princeton ^d	Dai <i>et al</i> (2003), Ji <i>et al</i> (2014)	Yes	Yes	Yes
JULES	Joint UK Land Environment Simulator model	WATCH (1901-2001) ^e	Best <i>et al</i> (2011)	Yes	Yes	Yes
ORCHIDEE-IPSL	Organising Carbon and Hydrology In Dynamic Ecosystems	WATCH (1901-1978) ^e	Gouttevin, I. <i>et al</i> (2012), Koven <i>et al</i> (2009), Krinner <i>et al</i> (2005)	Yes	Yes	Yes

LPJGUESS	Lund-Postdam-Jena dynamic global veg model	CRU TS 3.1 ^f	Gerten <i>et al</i> (2004), Wania <i>et al</i> (2009b, 2009a)	Yes	No	No
SiBCASA	Simple Biosphere/Carnegie-Ames-Stanford Approach model	CRUNCEP4 ^b	Schaefer <i>et al</i> (2011), Bonan (1996), Jafarov, E. and Schaefer (2016)	Yes	Yes	Yes
TEM604	Terrestrial Ecosystem Model	CRUNCEP4 ^b	Hayes <i>et al</i> (2014, 2011)	Yes	No	No
UW-VIC	Univ. of Washington Variable Infiltration Capacity model	CRU ^f , Udel ^h	Bohn <i>et al</i> (2013)	Internally calculated	Internally calculated	Yes

^aSimulations driven by temporal variability

^bViovy and Ciais (<http://dods.extra.cea.fr/>)

^cLong-wave dataset not from CRUNCEP4

^dSheffield *et al* (2006) (<http://hydrology.princeton.edu/data/pgf.php>)

^ehttp://www.eu-watch.org/gfx_content/documents/README-WFDEI.pdf

^fHarris *et al* (2014), University of East Anglia Climate Research Unit (2013)

^gMitchell and Jones (2005) for temperature

^hWillmott and Matsuura (2001) for wind speed and precipitation with corrections (see Bohn *et al.* 2013).

169 **Table 2. Hydrology and soil thermal characteristics of participating models.**

Model	Hydrology								Soil Thermal Properties			
	Evapotranspiration approach	Root water uptake	Infiltration	Water table	Soil Water Storage and Transmission	Groundwater Dynamics	Soil-ice impact	Snow	Soil thermal dynamics approach	Unfrozen Water effects on Phase Change	Moss insulation	Organic soil insulation
CLM 4.5	Sum of canopy evaporation, transpiration, and soil evaporation	Macroscopic approach	Saturation-excess runoff $F_{sat}=f(z_{wt})$	Niu et al. (2007); perched water table possible if ice layer present	Richard's equation (Clapp Hornberger functions)	Base flow from TOPMODEL concepts, unconfined aquifer (Niu et al. 2007)	Impacts hydrologic properties through power-law ice impedance (Swenson et al., 2012)	Multi-layer dynamic (5 max)	Multi-layer Finite Difference Heat Diffusion	Yes	No	Yes
CoLM	BATS and Philip's (1957)	Macroscopic approach	Saturation-excess runoff $F_{sat}=f(z_{wt})$	Simple TOPMODEL	Richard's equation (Clapp Hornberger functions)	Base flow from TOPMODEL	Impacts hydrologic properties through power-law ice impedance	Multi-layer dynamic (5 max)	Multi-layer Finite Difference Heat Diffusion	No	No	No
JULES	Sum of ET, soil evaporation and moisture storages (e.g. lakes, urban) minus surface resistance	Macroscopic approach	Saturation-excess runoff $F_{sat}=f(z_{wt})$ or $F_{sat}=f(\theta)$	TOPMODEL or Probability Distribution Model	Richard's equation (Clapp Hornberger/van Genuchten functions)	Base flow from TOPMODEL	Hydraulic conductivity and suction determined by unfrozen water content (Brooks and Corey functions)	Multi-layer dynamic (3 max)	Multi-layer Finite Difference Heat Diffusion	Yes	No	No
ORCHIDEE-IPSL	Sum of bare soil, interception loss and plant transpiration for different veg PFTs in grid cell.	Macroscopic approach, water uptake different among cell veg PFTs (de Rosnay and Polcher, 1998)	Saturation-excess runoff $F_{sat}=f(\theta)$	TOPMODEL	Richard's equation (van Genuchten functions)	None	"Drying=Freezing" approximation (Gouttevin et al 2012)	Multi-layer dynamic (7 max)	1D Fourier Solution	Yes	No	Yes
LPJ-GUESS	Sum of Interception loss, plant transpiration and evaporation from soil. Gerten et al (2004)	Fractional water uptake different soil layers according to prescribed root distribution. (Wania et al., 2009a,b)	Depends on soil moisture and layer thickness. Declines exponentially with soil moisture	Uniform, and only for wetland grid cell (Wania et al., 2009a,b)	Analog to Darcy's Law, percolation rate depends on soil texture conductivity and soil wetness (Haxelmeier and Prentice, 1996).	Base flow is based on the exponential function to estimate percolation rate	Impacts hydrologic properties through power-law ice impedance	Multi-layer dynamic (3 max)	Multi-layer Finite Difference Heat Diffusion	No	No	No
SIBCASA	Sum of ground evaporation, surface dew, canopy ET and canopy dew (Bonan, 1996)	Macroscopic approach	Infiltration approach in non-saturated porous media described by Darcy's law	Niu et al. (2007); perched water table possible if ice layer present	Richard's equation (Clapp Hornberger functions)	Base flow from TOPMODEL concepts, unconfined aquifer (Niu et al. 2007)	Impacts hydrologic properties through power-law ice impedance	Multi-layer dynamic (5 max)	Multi-layer Finite Difference Heat Diffusion	Yes	No	Yes
TEM-604	Jenson-Haise potential ET (PET, Jenson and Haise 1963). Actual ET is calculated based on PET, water availability and leaf mass.	Based on the proportion of actual ET to potential ET	Field capacity-excess runoff (Thornthwaite and Mather 1957)	none	one-layer bucket	none	none	Multi-layer dynamic (9 max)	Multi-layer Finite Difference Heat Diffusion	No	Yes	No
UW-VIC	Sum of canopy interception, veg. transpiration and soil evaporation (Liang et al. 1994)	Based on reference ET and soil wilting point	Saturation-excess runoff $F_{sat}=f(\theta)$	Microtopography γ	From infiltration rate and infiltration shape parameter (Liang et al. 1994). No lateral flow between model grids	Base flow from Arno model conceptualization (Francini and Pacciani 1991)	Impacts hydrologic properties through power-law ice impedance	Bulk-layer dynamic (2 max)	Multi-layer Finite Difference Solution	Yes	No	Yes

170
171

2. Results

172

173

3.1 Soil Moisture

174

175

176

177

178

179

180

181

182

183

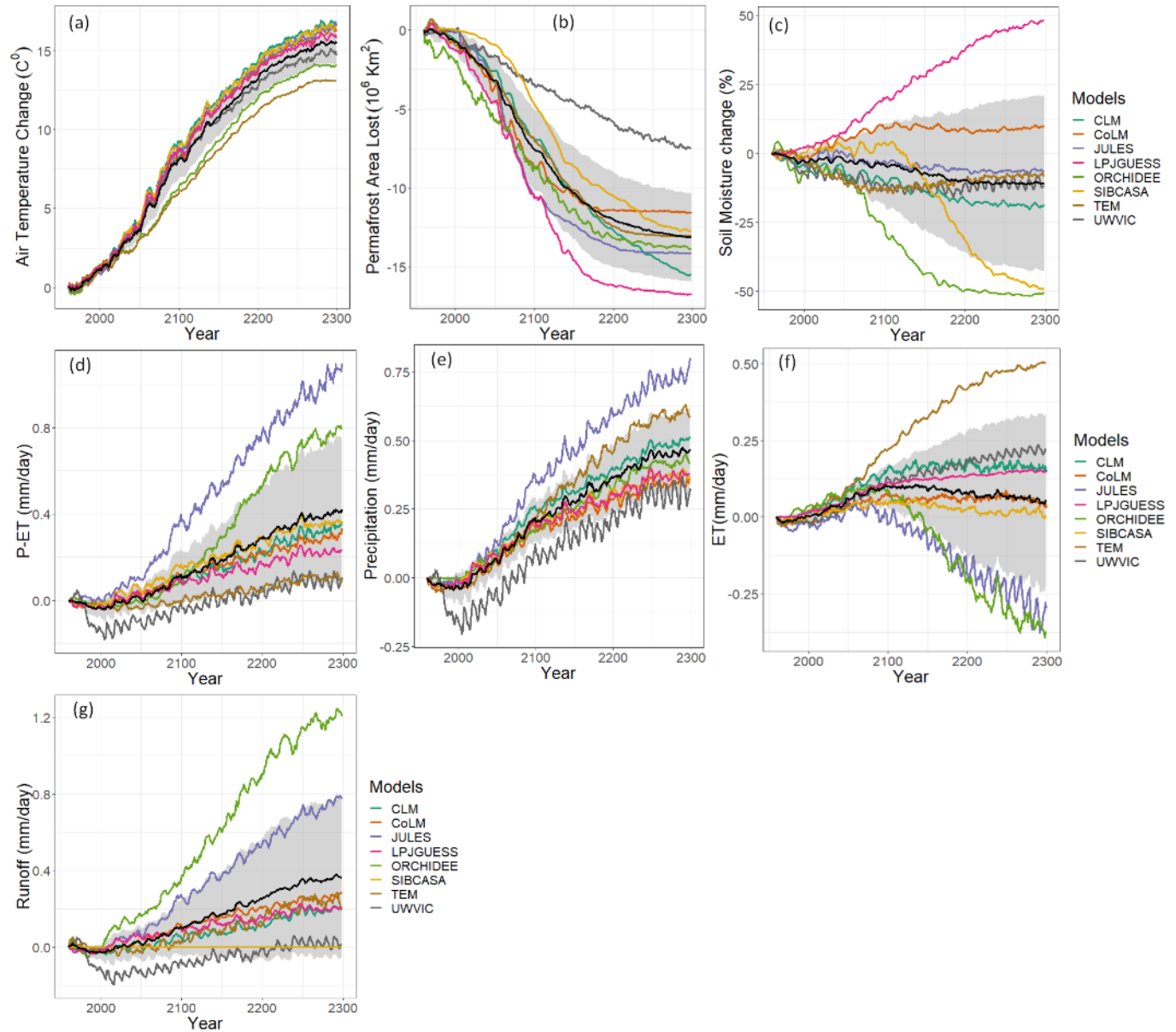
184

185

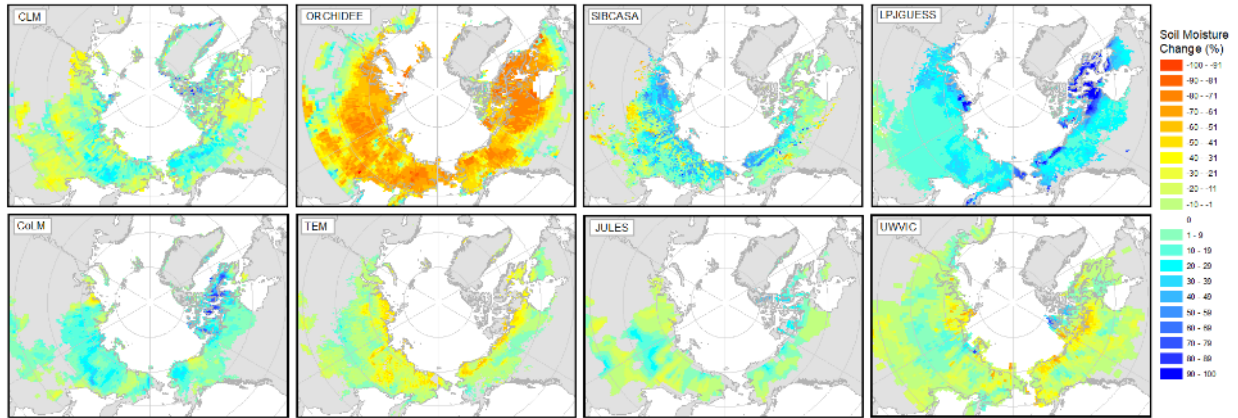
186

Air temperature forcing from greenhouse-gas emissions shows an increase of $\sim 15^{\circ}\text{C}$ in the permafrost domain over the simulation period (Figure 2a). With increases in air temperature, models project an ensemble mean decrease of ~ 13 million km^2 (91%) of the permafrost domain by 2299 (Figure 2b). Coincident with these changes, most models projected a long-term drying of the near-surface soils when averaged over the permafrost landscape (Figure 2c). However, the simulations diverged greatly with respect to both the permafrost-domain average soil moisture response and their associated spatial patterns (Figure 2c, 3). The models' ensemble mean indicated a change of -10% in near-surface soil moisture for the permafrost region by year 2299, but the spread across models was large. COLM and LPJGUESS simulate an increase in soil moisture of 10% and 48%, respectively. CLM, JULES, TEM6 and UWVIC exhibit qualitatively similar decreasing trends in soil moisture ranging between -5% and -20%. SIBCASA and ORCHIDEE projected a large soil moisture change of approximately -50% by 2299. Spatially,

187 models show diverse wetting and drying patterns and magnitudes across the permafrost zone (Figure 3).
 188 Several models tend to get wetter in the colder northern permafrost zones and are more susceptible to
 189 drying along the southern permafrost margin. Other models, such as TEM6 and UWVIC show the
 190 opposite pattern with drying more common in the northern part of the permafrost domain.
 191



192 **Figure 2. Simulated annual mean changes in air temperature, near-surface permafrost area, near-**
 193 **surface soil moisture and hydrology variables relative to 1960 (RCP 8.5). Annual mean is computed**
 194 **from monthly output values. The black line represents the models' ensemble mean and the gray**
 195 **area is the ensemble standard deviation. Figures d, e, f, and g are represented as change from 1960**
 196 **values. Time series are smoothed with a 7-year running mean for clarity and calculated over the**
 197 **initial permafrost domain of each model in 1960 for latitude >45°N.**
 198
 199
 200



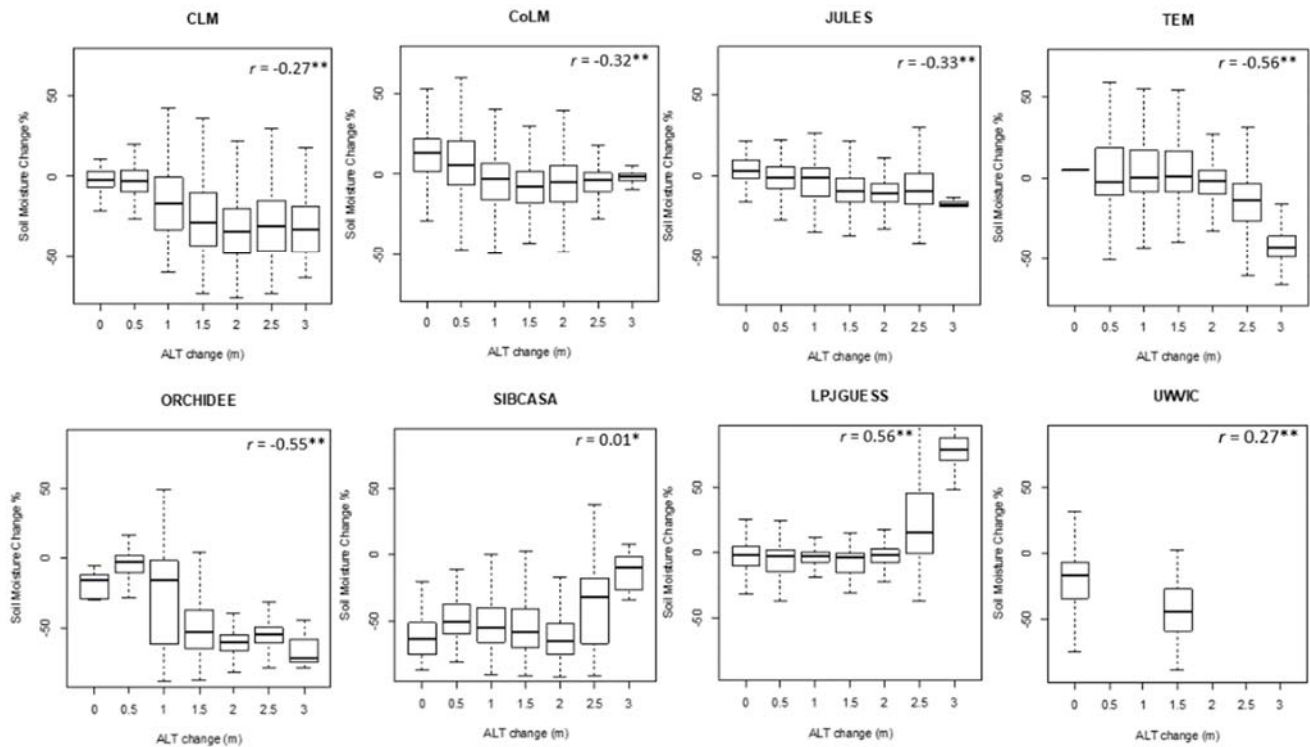
201
202
203
204
205
206
207

Figure 3. Spatial variability of projected changes in surface soil moisture (%) among models. Depicted changes are calculated as the difference between the 2071 to 2100 average and the 1960 to 1989 average. Colored area represents the initial simulated permafrost domain of 1960 for each model.

208 3.2 Drivers of Soil Moisture Change

209

210 To understand why models projected upper soil drying despite increases in the net precipitation (P-ET)
 211 into the soil, we examined whether or not increases in active layer thickness (ALT) and/or complete thaw
 212 of near-surface permafrost could be related to surface soil drying of the top 0-20cm ALT. We observed a
 213 general significant negative correlation in most models (except SIBCASA, LPJGUESS) where cells with
 214 greater increases in active layer thickness have greater drying (decrease) in near-surface soil moisture
 215 (Figure 4). However, there is a large spread between soil moisture and ALT changes (Figure 4). This
 216 spread may be influenced by many interacting factors that can be difficult to assess directly and are out of
 217 the scope of this study. In addition, the coarse soil column discretization in UWWIC limited this analysis
 218 for this model (Figure 1). However, most models show some indication that as the active layer deepens,
 219 soils tend to get drier at the surface.



220
221

222 **Figure 4. Responses of August near-surface (0-20cm) soil moisture to ALT changes. Each box**
 223 **represents a range of ± 0.25 m of ALT change. ALT and soil moisture change are calculated as the**
 224 **2290-2299 average minus the 1960-1989 average for cells in the initial permafrost domain of 1960.**
 225 **For cells where ALT exceeded 3 meters (no permafrost) during 2270-2299 period, we subtracted**
 226 **the initial active layer thickness (1960-1989 average) to 3 meters. Population Pearson correlations**
 227 **(r) significant at * $p < 0.01$ and ** $p < 2e-16$.**
 228

229 3.3 Precipitation, ET, and Runoff

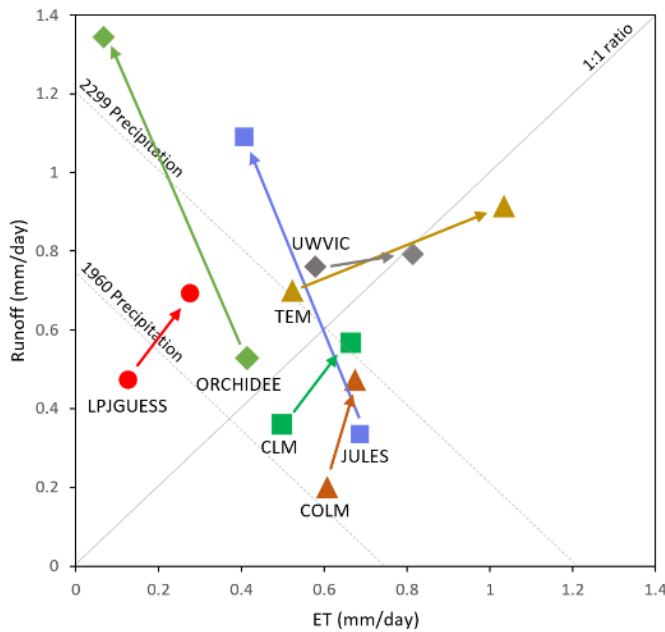
230

231 Models may project surface soil drying but the hydrological pathways through which this drying occurs
 232 appears to differ across models. The diversity of precipitation partitioning (Figure 5) demonstrates that
 233 specific representations and parameterizations for ET and runoff are not consistent across models. Though
 234 some models maintain a similar R/P ratio throughout the simulation (e.g., CLM, COLM, LPJGUESS),
 235 others show shifts from an ET-dominated system to a runoff-dominated system (e.g. JULES) and vice
 236 versa (e.g. TEM6 and UWVIC).

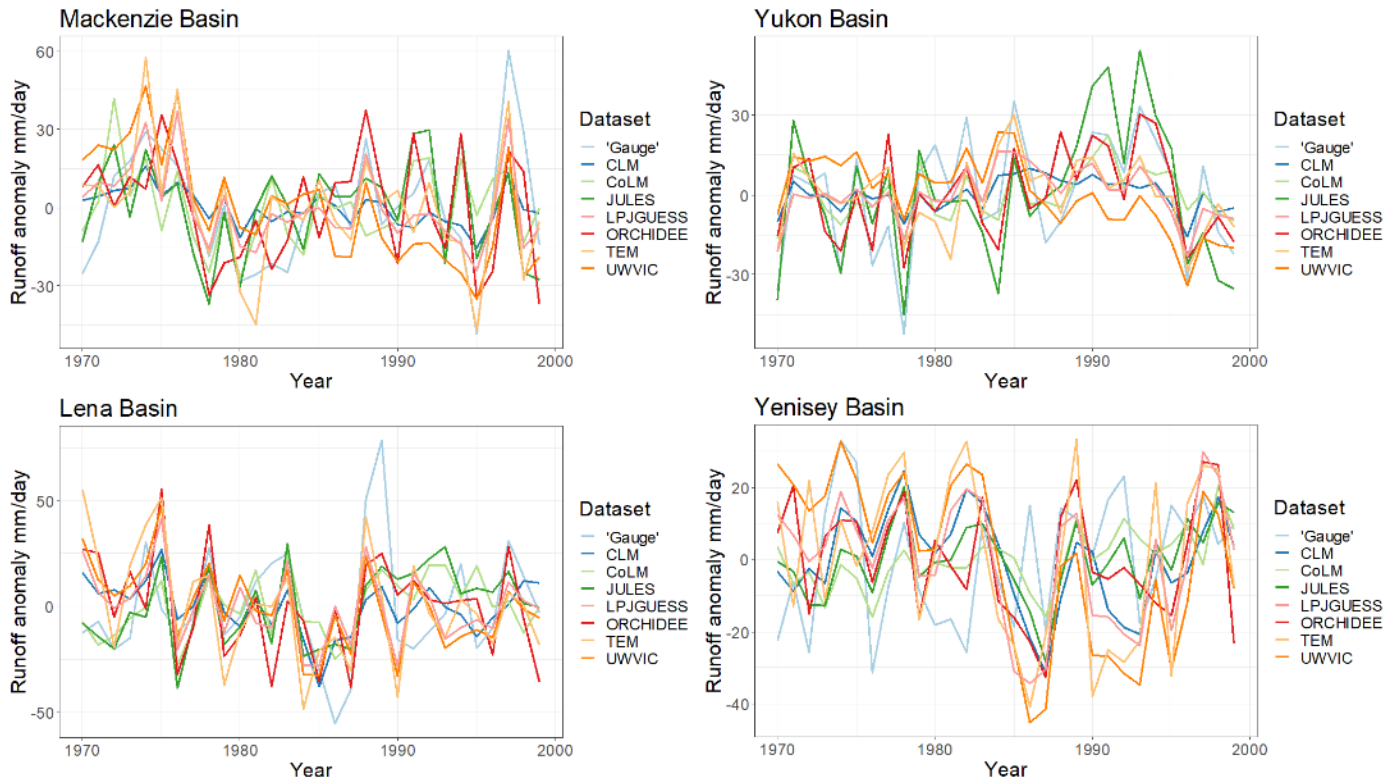
237 Evapotranspiration from the permafrost area is projected to rise in all models driven by warmer air
 238 temperatures and more productive vegetation, but the amplitude of that trend varies widely. The average
 239 projected evapotranspiration increase is 0.1 ± 0.1 mm/day (mean \pm SD, hereafter) by 2100, which
 240 represents about a 25% increase over 20th century levels. Beyond 2100, the ET projections diverge
 241 (Figure 2e).

242 Runoff is also projected to increase with projections across models being highly variable (Figure 2g). The
 243 change in the models' ensemble mean between 1960-2299 was 0.2 ± 0.2 mm/day. CLM, COLM,
 244 LPJGUESS and TEM6 simulated runoff changes of 0.2 to 0.3 mm/day by 2299. UWVIC exhibit small to
 245 null changes in runoff while SIBCASA shows surface runoff only.

246 Comparison between gauge station data and runoff simulations from the major river basins in the
 247 permafrost region shows that most models agree on the long term timing (Figure 6, Table 3) but the
 248 magnitude is generally underestimated (Figure 7). The gauge discharge mean for the four river basins is
 249 219 ± 36 mm/yr compared to the models' ensemble mean of 101 ± 82 mm/yr for the period 1970-1999.
 250 Excluding SIBCASA, the models' ensemble mean is 134 ± 69 mm/yr. However, models show reasonable
 251 correlations between runoff output and observed annual discharge time series (Table 3). SIBCASA
 252 horizontal subsurface runoff was disabled on the simulation because it tended to drain the active layer
 253 completely, resulting in very low and unrealistic soil moisture. Therefore, SIBCASA runoff values shown
 254 in this study are only for surface runoff.
 255 The net water balance (P-ET-R) is projected to increase for most models with precipitation increases
 256 outpacing the sum of ET and runoff changes. All models except TEM6 show an increase in the net water
 257 balance over the simulation period which suggests that models are collecting soil water deeper in the soil
 258 column, presumably in response to increasing ALT, even while the top soil layers dry.
 259
 260



261
 262
 263 **Figure 5. Precipitation partitioning between total runoff and evapotranspiration for participating**
 264 **models. Markers and arrows indicate the change from initial period (1960-1989 average) to final**
 265 **period (2270-2299 average). Diagonal dashed lines represent the ensemble rainfall mean for the**
 266 **initial (0.74 mm/day) and final (1.2 mm/day) simulation years. At any point along the dashed**
 267 **diagonals, runoff and ET sum to precipitation.**
 268
 269
 270

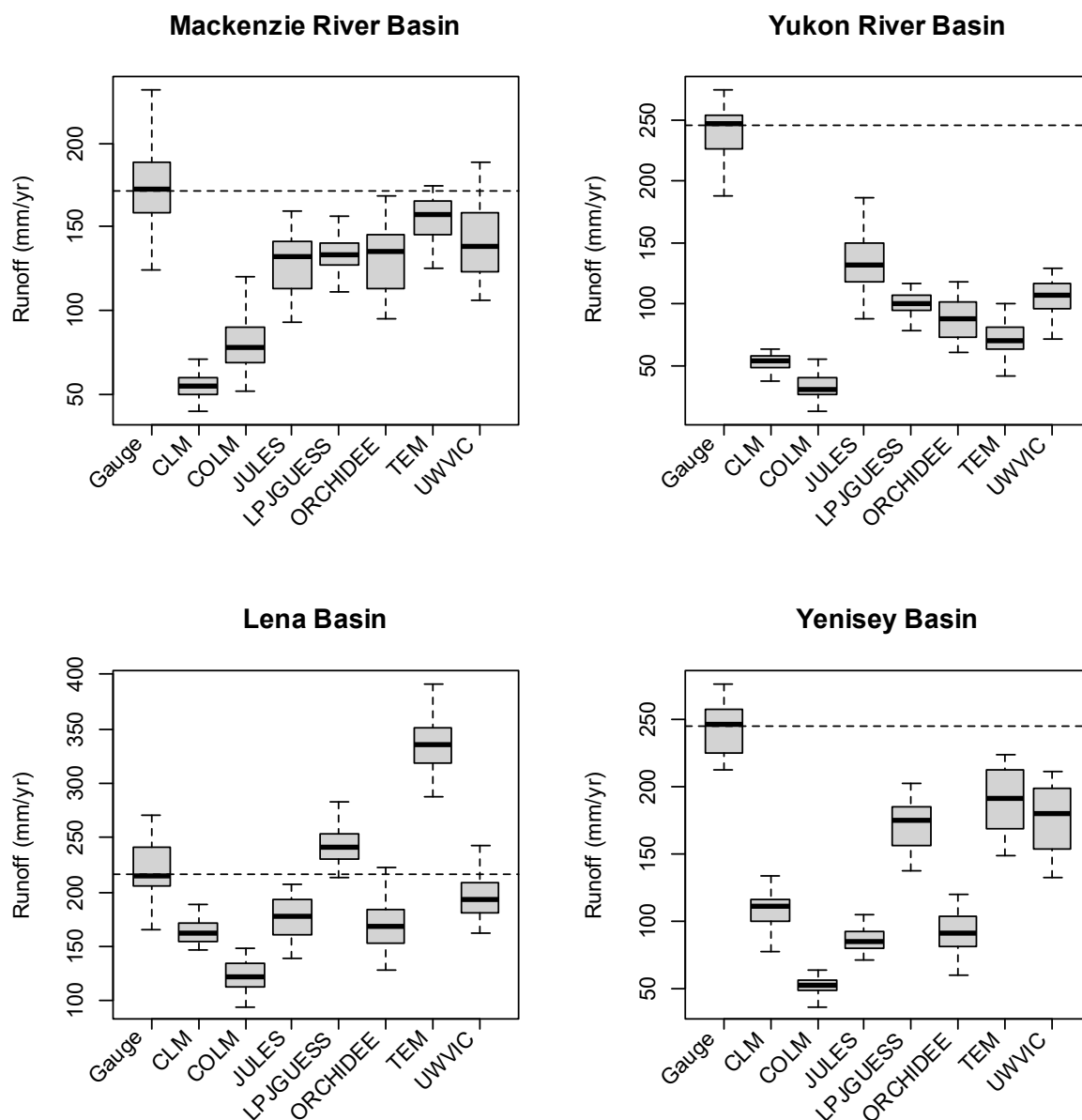


271
 272 **Figure 6. Runoff anomaly comparison between gauge data and models simulations for the period**
 273 **1970-1999.**

274
 275 **Table 3. Correlation coefficients between simulated annual total runoff and gauge mean annual**
 276 **discharge 1970 to 1999. SIBCASA correlations are for surface runoff.**

Model	River Basin				Avg.
	Mackenzie	Yukon	Yenisey	Lena	
CLM	0.70	0.64	0.08	0.46	0.47
ORCHIDEE	0.57	0.69	0.36	0.37	0.50
LPJGGUESS	0.68	0.71	0.14	0.35	0.47
TEM	0.66	0.56	0.16	0.40	0.45
SIBCASA	0.49	0.21	0.08	0.29	0.27
JULES	0.41	0.77	0.34	0.51	0.51
COLM	0.38	0.76	0.27	0.46	0.47
UWVIC	0.44	0.38	0.02	0.31	0.29
Avg.	0.54	0.59	0.18	0.40	

277



278
 279 **Figure 7. Discharge comparison between gauge station data and model output for each river basin.**
 280 **Dashed line indicates mean annual discharge at gauge station. Boxplots derived from mean annual**
 281 **discharge (total runoff) simulations for the period of 1970 to 1999.**

282
 283 **4. Discussion**

284
 285 This study assessed near-surface soil moisture and hydrology projections in the permafrost region using
 286 widely-used land models that represent permafrost. Most models showed near-surface drying despite the
 287 externally-forced intensification of the water cycle driven by climate change. Drying was generally
 288 associated with increases of active layer thickness and permafrost degradation in a warming climate. We
 289 show that the timing and magnitude of projected soil moisture changes vary widely across models,

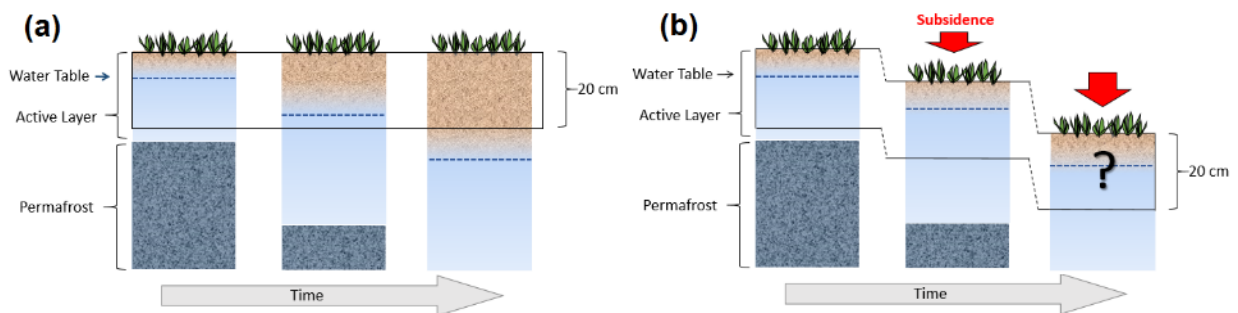
290 pointing to an uncertain future in permafrost hydrology and associated climatic feedbacks. In this section,
291 we review the role of projected permafrost loss and active layer thickening on soil moisture changes and
292 some potential sources of variability among models. In addition, we comment on the potential effects of
293 soil moisture projections on the permafrost carbon-climate feedback. It is important to note that this study
294 is more qualitative in nature and does not focus on the detail of magnitude or spatial patterns of model
295 signatures.

296

297 4.1 Permafrost degradation and drying

298

299 Increases in net precipitation and the counterintuitive drying of the top soil in the permafrost region
300 suggests that soil column processes such as changes in active layer thickness (ALT) and activation of
301 subsurface drainage with permafrost thaw are acting to dry the top soil layers (Figure 8a). In general,
302 models represent impermeable soils when frozen. Then, as soils thaw at progressively depths in the
303 summer, liquid water infiltrates further into the active layer draining deeper into the thawed soil column
304 (Avis et al., 2011; Lawrence et al., 2015; Swenson et al., 2012). However, relevant soil column processes
305 related to thermokarst by thawing of excess ground ice (Lee et al., 2014) are limited in these simulations
306 despite their significant occurrence in the permafrost region (Olefeldt et al., 2016). As permafrost thaws,
307 ground ice melts, potentially reducing the volume of the soil column and changing the hydrological
308 properties of the soil (Aas et al., 2019; Nitzbon et al., 2019). This would occur where soil surface
309 elevation drops through sudden collapse or slow deformation by an amount equal to or greater than the
310 increased depth of annual thaw (Figure 8b). This mechanism, not represented in current large-scale
311 models, could result in projected increases or no change in the water table over time as observed by long-
312 term studies (Andresen and Loughheed, 2015; Mauritz et al., 2017; Natali et al., 2015). Subsidence of 12-
313 13 cm has been observed in Northern Alaska over a five year period, which represents a volume loss of
314 about 25% of the average ALT for that region (~50cm) (Streletskiy et al., 2008). These lines of evidence
315 may suggest that permafrost thaw may not dry the Arctic as fast as simulated by land models but rather
316 maintain or enhanced soil water saturation depending on the water balance of the modeled cell column.
317



318

319 **Figure 8. Schematic of changes in the soil column moisture (a) without subsidence (current models)**
320 **and (b) with subsidence from thawing ice-rich permafrost (not represented by models), a process**
321 **that may accumulate soil moisture and slow down drying over time.**

322

323 Recent efforts have been made to address the high sub-grid heterogeneity of fine-scale mechanisms
324 including soil subsidence (Aas et al., 2019), hillslope hydrology, talik and thermokarst development
325 (Jafarov et al., 2018), ice wedge degradation (Abolt et al., 2018; Liljedahl et al., 2016; Nitzbon et al.,
326 2019), vertical and lateral heat transfer on permafrost thaw and groundwater flow (Kurylyk et al., 2016)

327 and lateral water fluxes (Nitzbon et al., 2019). These processes are known to have a major role on surface
328 and subsurface hydrology and their implementation in large scale models is needed. Other important
329 challenges in land models' hydrology include representation of the significant area dynamics of the
330 ubiquitous smaller, shallow water bodies observed over recent decades (Andresen and Loughheed, 2015;
331 Jones et al., 2011; Roach et al., 2011; Smith et al., 2005). These systems are either lacking in simulations
332 (polygon ponds and small lakes) or assumed to be static systems in simulations (large lakes). The
333 implementation of surface hydrology dynamics and permafrost processes in large-scale land models will
334 help reduce uncertainty in our ability to predict the future hydrological state of the Arctic and the
335 associated climatic feedbacks. It is important to note that all these processes require data for model
336 calibration, verification and evaluation, that is commonly absent at large scales. Permafrost hydrology
337 will only advance through synergistic efforts between field researchers and modelers.

338

339 **4.2 Uncertainty in soil moisture and hydrology simulations**

340 Differences in representations of soil thermal dynamics can directly affect hydrology through timing of
341 the freezing-thawing cycle and by altering the rates of permafrost loss and subsurface drainage (Finney et
342 al., 2012). McGuire et al. (2016) and Peng et al. (2016) show that these models exhibit considerable
343 differences in permafrost quantities such as active layer thickness, and the mean and trends in near-
344 surface (0-3m) permafrost extent, even though all the models are forced with observed climatology.
345 However, these differences are smaller than those seen across the CMIP5 models (Koven et al., 2013). All
346 models except ORCHIDEE employ a multi-layer finite difference heat diffusion for soil thermal
347 dynamics (Table 2). Organic soil insulation, snow insulation, and unfrozen water effects on phase change
348 are the most common structural differences among models for soil thermal dynamics but do not explain
349 the variability in the simulated changes in ALT and permafrost area as shown by McGuire *et al* (2016).
350 Half of the participating models include organic matter in the soil properties (CLM, ORCHIDEE,
351 SIBCASA, UWVIC) which can significantly impact soil thermal properties and lead to an increase in the
352 hydraulic conductivity of the soil column, thereby enhancing drainage and redistribution of water in the
353 soil column. Soil vertical characterization is another important aspect for soil thermal dynamics and
354 hydrology (Chadburn et al., 2015; Nicolsky et al., 2007). Lawrence et al (2008) indicated that a high-
355 resolution soil column representation is necessary for accurate simulation of long term trends in active
356 layer depth. However, McGuire *et al* (2016) showed that soil column depth did not clearly explain
357 variability of the simulated loss of permafrost area across models.

358 Water table representation can result in a first order effect on soil moisture. Most models (CLM, COLM,
359 SIBCASA and ORCHIDEE) use some version of TOPMODEL (Niu et al., 2007), which employs a
360 prognostic water table where sub-grid scale topography is the main driver of soil moisture variability in
361 the cell. However, water table is not explicitly represented in other models such as LPJGUESS, which has
362 a uniform water table which is only applied for wetland areas. In addition to water table, storage and
363 transmission of water in soils is a fundamental component of an accurate representation of soil moisture
364 (Niu and Yang, 2006). The representation of soil water storage and transmission varies across models
365 from Richards equations based on Clapp Hornberger and/or van Genuchten (1980) functions (e.g CLM,
366 CoLM, SIBCASA, ORCHIDEE) to a simplified one layer bucket (e.g. TEM6). It is also important to
367 note that most models differ in their numerical implementations of processes, such as water movement
368 through frozen soils (Gouttevin, I. et al., 2012; Swenson et al., 2012), and in the use of iterative solutions
369 and vertical discretization of water transmission (De Rosnay et al., 2000).

370 Differences in representation of vertical fluxes through evapotranspiration (ET) are also likely adding to
371 the high variability in soil moisture projections. ET sources (e.g. interception loss, plant transpiration, soil
372 evaporation) were similar across models but had different formulations (Table 2). The diversity of ET
373 implementations (e.g. evaporative resistances from fractional areas, etc.) and of vegetation maps used by
374 the modelling groups (Ottlé et al., 2013) can also contribute to the big spread on the temporal simulations
375 for ET and soil moisture. Along with projected increases in ET, net precipitation (P-ET) is projected to
376 increase for all models suggesting that drying is not attributed only to soil evaporation, and the increasing
377 net water balance (P-ET-R) proposes that models are storing water deeper in the soil column as
378 permafrost near the surface thaws.

379 Despite runoff improvements (Swenson et al., 2012), underestimation of river discharge has been a
380 challenge in previous versions in models (Slater et al., 2007). The differences between models and
381 observations in mean annual discharge may stem from several sources. Particularly, the substantial
382 variation in the precipitation forcing for these models (Figure 2e). This is attributed, in part, to the sparse
383 observational networks in high latitudes. River discharge at high latitudes can differ substantially when
384 different reanalysis forcing datasets are used. For example, river discharge for Arctic rivers differs
385 substantially in CLM4.5 simulations when forced with GSWP3v1 compared to CRUNCEPv7 reanalysis
386 datasets (not shown, runoff for MacKenzie, +32%; Yukon, +78%; Lena, -2%; Yenisey, +22%). Other
387 factors include potential deficiencies in the parameterization and/or implementation of ET and runoff
388 processes as well as vegetation processes.

389

390 **4.3 Implications for the permafrost carbon-climate feedback**

391

392 If drying of the permafrost region occurs, carbon losses from the soil will be dominated by CO₂ as a result
393 of increased heterotrophic respiration rates compared to moist conditions (Elberling et al., 2013;
394 Oberbauer et al., 2007; Schädel et al., 2016). With projected drying, CH₄ flux emissions will slow down
395 by the reduction of soil saturation and inundated areas through lowering the water table in grid cells
396 (Figure 8A). In a sensitivity study using CLM, the slower increase of methane emissions associated with
397 surface drying could potentially lead to a reduction in the Global Warming Potential of permafrost carbon
398 emissions by up to 50% compared to saturated soils (Lawrence et al., 2015). However, we need to also
399 consider that current land models lack representation of important CH₄ sources and pathways in the
400 permafrost region such as lake and wetland dynamics that can counteract the suppression of CH₄ fluxes
401 by projected drying. Seasonal wetland area variation, which is not represented or is poorly represented in
402 current models, can contribute to a third of the annual CH₄ flux in boreal wetlands (Ringeval et al., 2012).
403 Although this manuscript may raise more questions than answers, this study highlights the importance of
404 advancing hydrology and hydrological heterogeneity in land models to help determine the spatial
405 variability, timing, and reasons for changes in hydrology of terrestrial landscapes of the Arctic. These
406 improvements may constrain projections of land-atmosphere carbon exchange and reduce uncertainty on
407 the timing and intensity of the permafrost carbon feedback.

408

409 **Data availability**

410

411 The simulation data analyzed in this manuscript is available through the National Snow and Ice Data
412 Center (NSIDC; <http://nsidc.org>). Inquires please contact Kevin Schaefer (kevin.schaefer@nsidc.org).

413

414 **Author contributions**

415

416 This manuscript is a collective effort of the modeling groups of the Permafrost Carbon Network
417 (<http://www.permafrostcarbon.org>). C.G.A, D.M.L., C.J.W., A.D.M. wrote the initial draft with additional
418 contributions of all authors. Figures prepared by C.G.A.

419

420 **Acknowledgements**

421

422 This manuscript is dedicated to the memory of Andrew G. Slater (1971 -2016) for his scientific
423 contributions in advancing Arctic hydrology modeling. This work was performed under the Next-
424 Generation Ecosystem Experiments (NGEE Arctic, DOE ERKP757) project supported by the Office of
425 Biological and Environmental Research in the U.S. Department of Energy, Office of Science. The study
426 was also supported by the National Science Foundation through the Research Coordination Network
427 (RCN) program and through the Study of Environmental Arctic Change (SEARCH) program in support
428 of the Permafrost Carbon Network. We also acknowledge the joint DECC/Defra Met Office Hadley
429 Centre Climate Programme (GA01101) and the European Union FP7-ENVIRONMENT project PAGE21.

430

431 **References**

432

433 Aas, K. S., Martin, L., Nitzbon, J., Langer, M., Boike, J., Lee, H., Berntsen, T. K. and Westermann, S.:
434 Thaw processes in ice-rich permafrost landscapes represented with laterally coupled tiles in a land surface
435 model, *Cryosphere*, 13(2), 591–609, doi:10.5194/tc-13-591-2019, 2019.

436 Abolt, C. J., Young, M. H., Atchley, A. L. and Harp, D. R.: Microtopographic control on the ground
437 thermal regime in ice wedge polygons, *Cryosphere*, 12(6), 1957–1968, doi:10.5194/tc-12-1957-2018,
438 2018.

439 Andresen, C. G. and Lougheed, V. L.: Disappearing arctic tundra ponds: Fine-scale analysis of surface
440 hydrology in drained thaw lake basins over a 65 year period (1948-2013)., *J. Geophys. Res.*, 120, 1–14,
441 doi:10.1002/2014JG002778, 2015.

442 Andresen, C. G., Lara, M. J., Tweedie, C. T. and Lougheed, V. L.: Rising plant-mediated methane
443 emissions from arctic wetlands, *Glob. Chang. Biol.*, 23(3), 1128–1139, doi:10.1111/gcb.13469, 2017.

444 Avis, C. a., Weaver, A. J. and Meissner, K. J.: Reduction in areal extent of high-latitude wetlands in
445 response to permafrost thaw, *Nat. Geosci.*, 4(7), 444–448, doi:10.1038/ngeo1160, 2011.

446 Best, M. J., Pryor, M., Clark, D. B., Rooney, G. G., Essery, R. L. H., Menard, C. B., Edwards, J. M.,
447 Hendry, M. a., Porson, a., Gedney, N., Mercado, L. M., Sitch, S., Blyth, E., Boucher, O., Cox, P. M.,
448 Grimmond, C. S. B. and Harding, R. J.: The Joint UK Land Environment Simulator (JULES), model
449 description. Part 1: Energy and water fluxes, *Geosci. Model Dev.*, 4, 677–699, doi:10.5194/gmdd-4-641-
450 2011, 2011.

451 Bohn, T. J., Podest, E., Schroeder, R., Pinto, N., McDonald, K. C., Glagolev, M., Filippov, I., Maksyutov,
452 S., Heimann, M., Chen, X. and Lettenmaier, D. P.: Modeling the large-scale effects of surface moisture
453 heterogeneity on wetland carbon fluxes in the West Siberian Lowland, *Biogeosciences*, 10(10), 6559–
454 6576, doi:10.5194/bg-10-6559-2013, 2013.

455 Bonan, G. B.: A Land Surface Model (LSM v1.0) for Ecological, Hydrological and Atmospheric studies:
456 Technical descripton and user’s guide., 1996.

457 Chadburn, S. E., Burke, E. J., Essery, R. L. H., Boike, J., Langer, M., Heikenfeld, M., Cox, P. M. and
458 Friedlingstein, P.: Impact of model developments on present and future simulations of permafrost in a
459 global land-surface model, *Cryosphere*, 9(4), 1505–1521, doi:10.5194/tc-9-1505-2015, 2015.

460 Dai, Y., Zeng, X., Dickinson, R. E., Baker, I., Bonan, G. B., Bosilovich, M. G., Denning, A. S., Dirmeyer
461 P, Houser, P. R., Niu, G., Oleson, K. W., Schlosser, C. A. and Yang, Z.: The Common Land Model

462 (CoLM), *Bull. Am. Meteorol. Soc.*, 84, 1013–1023, doi:10.1175/BAMS-84-8-1013, 2003.

463 Elberling, B., Michelsen, A., Schädel, C., Schuur, E. A. G., Christiansen, H. H., Berg, L., Tamstorf, M. P.

464 and Sigsgaard, C.: Long-term CO₂ production following permafrost thaw, *Nat. Clim. Chang.*, 3(October),

465 890–894, doi:10.1038/nclimate1955, 2013.

466 Finney, D. L., Blyth, E. and Ellis, R. .: Improved modelling of Siberian river flow through the use of an

467 alternative frozen soil hydrology scheme in a land surface model, *Cryosph.*, 6, 859–870,

468 doi:https://doi.org/10.5194/tc-6-859-2012, 2012.

469 Francini, M. and Paciani, M.: Comparative analysis of several conceptual rainfall-runoff models, *J.*

470 *Hydrol.*, 122, 161–219, 1991.

471 Frey, K. E. and McClelland, J. W.: Impacts of permafrost degradation on arctic river biogeochemistry,

472 *Hydrol. Process.*, 23, 169–182, doi:10.1002/hyp, 2009.

473 Gent, P. R., Danabasoglu, G., Donner, L. J., Holland, M. M., Hunke, E. C., Jayne, S. R., Lawrence, D.

474 M., Neale, R. B., Rasch, P. J., Vertenstein, M., Worley, P. H., Yang, Z. L. and Zhang, M.: The

475 community climate system model version 4, *J. Clim.*, 24(19), 4973–4991, doi:10.1175/2011JCLI4083.1,

476 2011.

477 Gerten, D., Schaphoff, S., Haberlandt, U., Lucht, W. and Sitch, S.: Terrestrial vegetation and water

478 balance — hydrological evaluation of a dynamic global vegetation model, , 286, 249–270,

479 doi:10.1016/j.jhydrol.2003.09.029, 2004.

480 Gouttevin, I., Krinner, G., Ciais, P., Polcher, J. and Legout, C.: Multi-scale validation of a new soil

481 freezing scheme for a land-surface model with physically-based hydrology, *Cryosph.*, 6, 407–430, 2012.

482 Grosse, G., Jones, B. and Arp, C.: Thermokarst lakes, drainage, and drained basins, in *Treatise on*

483 *Geomorphology*, vol. 8, pp. 325–353., 2013.

484 Harris, I., Jones, P. D., Osborn, T. J. and Lister, D. H.: Updated high-resolution grids of monthly climatic

485 observations - the CRU TS3.10 Dataset, *Int. J. Climatol.*, 34(3), 623–642, doi:10.1002/joc.3711, 2014.

486 Haxeltine, A. and Prentice, I. C.: A General Model for the Light-Use Efficiency of Primary Production,

487 *Funct. Ecol.*, 10(5), 551–561, 1996.

488 Hayes, D. J., McGuire, A. D., Kicklighter, D. W., Gurney, K. R., Burnside, T. J. and Melillo, J. M.: Is the

489 northern high - latitude land - based CO₂ sink weakening ?, *Global Biogeochem. Cycles*, 25(May), 1–14,

490 doi:10.1029/2010GB003813, 2011.

491 Hayes, D. J., Kicklighter, D. W., McGuire, a D., Chen, M., Zhuang, Q., Yuan, F., Melillo, J. M. and

492 Wullschleger, S. D.: The impacts of recent permafrost thaw on land–atmosphere greenhouse gas

493 exchange, *Environ. Res. Lett.*, 9(4), 045005, doi:10.1088/1748-9326/9/4/045005, 2014.

494 Jafarov, E. and Schaefer, K.: The importance of a surface organic layer in simulating permafrost thermal

495 and carbon dynamics, *Cryosph.*, 10, 465–475, doi:10.5194/tc-10-465-2016, 2016, 2016.

496 Jafarov, E. E., Coon, E. T., Harp, D. R., Wilson, C. J., Painter, S. L., Atchley, A. L. and Romanovsky, V.

497 E.: Modeling the role of preferential snow accumulation in through talik development and hillslope

498 groundwater flow in a transitional permafrost landscape, *Environ. Res. Lett.*, 13(10), doi:10.1088/1748-

499 9326/aadd30, 2018.

500 Jensen, M. E. and Haise, H. R.: Estimating evapotranspiration from solar radiation, *J. Irrig. Drain. Div.*

501 *ASCE*, (89), 15–41, 1963.

502 Ji, D., Wang, L., Feng, J., Wu, Q., Cheng, H., Q, Z., Yang, J., Dong, W., Dai, Y., Gong, D., Zhang, R. H.,

503 Wang, X., Liu, J., Moore, J. C., Chen, D. and Zhou, M.: Description and basic evaluation of Beijing

504 Normal University Earth system model (BNU-ESM) version 1, *Geosci. Model Dev.*, 7, 2039–2064, 2014.

505 Jones, B. M., Grosse, G., Arp, C. D., Jones, M. C., Walter Anthony, K. M. and Romanovsky, V. E.:

506 Modern thermokarst lake dynamics in the continuous permafrost zone, northern Seward Peninsula,

507 Alaska, *J. Geophys. Res.*, 116, G00M03, doi:10.1029/2011JG001666, 2011.

508 Kanevskiy, M., Shur, Y., Jorgenson, T., Brown, D. R. N., Moskalenko, N., Brown, J., Walker, D. A.,

509 Reynolds, M. K. and Buchhorn, M.: Degradation and stabilization of ice wedges: Implications for

510 assessing risk of thermokarst in northern Alaska, *Geomorphology*, 297, 20–42,

511 doi:10.1016/j.geomorph.2017.09.001, 2017.

512 Koven, C., Friedlingstein, P., Ciais, P., Khvorostyanov, D., Krinner, G. and Tarnocai, C.: On the

513 formation of high-latitude soil carbon stocks: Effects of cryoturbation and insulation by organic matter in
514 a land surface model, *Geophys. Res. Lett.*, 36(21), 1–5, doi:10.1029/2009GL040150, 2009.

515 Koven, C. D., Riley, W. J. and Stern, A.: Analysis of permafrost thermal dynamics and response to
516 climate change in the CMIP5 earth system models, *J. Clim.*, 26(6), 1877–1900, doi:10.1175/JCLI-D-12-
517 00228.1, 2013.

518 Koven, C. D., Lawrence, D. M. and Riley, W. J.: Permafrost carbon–climate feedback is sensitive to deep
519 soil carbon decomposability but not deep soil nitrogen dynamics, *Proc. Natl. Acad. Sci.*, 201415123,
520 doi:10.1073/pnas.1415123112, 2015.

521 Krinner, G., Viovy, N., de Noblet-Ducoudré, N., Ogée, J., Polcher, J., Friedlingstein, P., Ciais, P., Sitch,
522 S. and Prentice, I. C.: A dynamic global vegetation model for studies of the coupled atmosphere-
523 biosphere system, *Global Biogeochem. Cycles*, 19(1), 1–33, doi:10.1029/2003GB002199, 2005.

524 Kurylyk, B. L., Hayashi, M., Quinton, W. L., McKenzie, J. M. and Voss, C. I.: Influence of vertical and
525 lateral heat transfer on permafrost thaw, peatland landscape transition, and groundwater flow, *Water
526 Resour. Res.*, 52(2), 1286–1305, doi:10.1002/2015WR018057, 2016.

527 Lara, M. J., McGuire, A. D., Euskirchen, E. S., Tweedie, C. E., Hinkel, K. M., Skurikhin, A. N.,
528 Romanovsky, V. E., Grosse, G., Bolton, W. R. and Genet, H.: Polygonal tundra geomorphological change
529 in response to warming alters future CO₂ and CH₄ flux on the Barrow Peninsula, *Glob. Chang. Biol.*,
530 21, 1663–1651, doi:10.1111/gcb.12757, 2015.

531 Lawrence, D. M., Slater, A. G., Romanovsky, V. E. and Nicolsky, D. J.: Sensitivity of a model projection
532 of near-surface permafrost degradation to soil column depth and representation of soil organic matter, *J.
533 Geophys. Res.*, 113(F2), F02011, doi:10.1029/2007JF000883, 2008.

534 Lawrence, D. M., Koven, C. D., Swenson, S. C., Riley, W. J. and Slater, A. G.: Permafrost thaw and
535 resulting soil moisture changes regulate projected high-latitude CO₂ and CH₄ emissions, *Environ. Res.
536 Lett.*, 10(9), 094011, doi:10.1088/1748-9326/10/9/094011, 2015.

537 Lee, H., Swenson, S. C., Slater, A. G. and Lawrence, D. M.: Effects of excess ground ice on projections
538 of permafrost in a warming climate, *Environ. Res. Lett.*, 9(12), 124006, doi:10.1088/1748-
539 9326/9/12/124006, 2014.

540 Liang, X., Lettenmaier, D. P., Wood, E. F. and Burges, S.: A simple hydrologically based model of land
541 surface water and energy fluxes for general circulation models, *J. Geophys. Res.*, 99(D7), 14415–14418,
542 1994.

543 Liljedahl, A., Boike, J., Daanen, R. P., Fedorov, A. N., Frost, G. V., Grosse, G., Hinzman, L. D., Iijma,
544 Y., Jorgenson, J. C., Matveyeva, N., Necsoiu, M., Reynolds, M. K., Romanovsky, V., Schulla, J., Tape,
545 K. D., Walker, D. A., Wilson, C., Yabuki, H. and Zona, D.: Pan-Arctic ice-wedge degradation in warming
546 permafrost and influence on tundra hydrology, *Nat. Geosci.*, 9(April), 312–319, doi:10.1038/ngeo2674,
547 2016.

548 Mauritz, M., Bracho, R., Celis, G., Hutchings, J., Natali, S. M., Pegoraro, E., Salmon, V. G., Schädel, C.,
549 Webb, E. E. and Schuur, E. A. G.: Nonlinear CO₂ flux response to 7 years of experimentally induced
550 permafrost thaw, *Glob. Chang. Biol.*, 23(9), 3646–3666, doi:10.1111/gcb.13661, 2017.

551 McGuire, A. D., Lawrence, D. M., Koven, C., Clein, J. S., Burke, E., Chen, G., Jafarov, E., MacDougall,
552 A. H., Marchenko, S., Nicolsky, D., Peng, S., Rinke, A., Ciais, P., Gouttevin, I., Hayes, D. J., Ji, D.,
553 Krinner, G., Moore, J. C., Romanovsky, V., Schädel, C., Schaefer, K., Schuur, E. A. G. and Zhuang, Q.:
554 The Dependence of the Evolution of Carbon Dynamics in the Northern Permafrost Region on the
555 Trajectory of Climate Change, *Proc. Natl. Acad. Sci.*, 2018.

556 McGuire, D. A., Koven, C. D., Lawrence, D. M., Burke, E., Chen, G., Chen, X., Delire, C. and Jafarov,
557 E.: Variability in the sensitivity among model simulations of permafrost and carbon dynamics in the
558 permafrost region between 1960 and 2009, *Global Biogeochem. Cycles*, 1–23,
559 doi:10.1002/2016GB005405. Received, 2016.

560 Mitchell, T. D. and Jones, P. D.: An improved method of constructing a database of monthly climate
561 observations and associated high-resolution grids, *Int. J. Climatol.*, 25(6), 693–712, doi:10.1002/joc.1181,
562 2005.

563 Natali, S. M., Schuur, E. a G., Mauritz, M., Schade, J. D., Celis, G., Crummer, K. G., Johnston, C.,

564 Krapek, J., Pegoraro, E., Salmon, V. G. and Webb, E. E.: Permafrost thaw and soil moisture driving CO₂
565 and CH₄ release from upland tundra, *J. Geophys. Res. Biogeosciences*, 120, 525–537,
566 doi:10.1002/2014JG002872. Received, 2015.

567 Newman, B. D., Throckmorton, H. M., Graham, D. E., Gu, B., Hubbard, S. S., Liang, L., Wu, Y.,
568 Heikoop, J. M., Herndon, E. M., Phelps, T. J., Wilson, C. J. and Wulfschleger, S. D.: Microtopographic
569 and depth controls on active layer chemistry in Arctic polygonal ground, *Geophys. Res. Lett.*, 42(6),
570 1808–1817, doi:10.1002/2014GL062804, 2015.

571 Nicolsky, D. J., Romanovsky, V. E., Alexeev, V. A. and Lawrence, D. M.: Improved modeling of
572 permafrost dynamics in a GCM land-surface scheme, *Geophys. Res. Lett.*, 34,
573 doi:10.1029/2007GL029525, 2007.

574 Nitzbon, J., Langer, M., Westerman, S., Martin, L., Schanke Aas, K. and Boike, J.: Modelling the
575 degradation of ice-wedges in polygonal tundra under different hydrological conditions, *Cryosph.*, 13,
576 1089–1123, 2019.

577 Niu, G.-Y., Yang, Z.-L., Dickinson, R. E., Gulden, L. E. and Su, H.: Development of a simple
578 groundwater model for use in climate models and evaluation with Gravity Recovery and Climate
579 Experiment data, *J. Geophys. Res.*, 112(D7), D07103, doi:10.1029/2006JD007522, 2007.

580 Niu, G. and Yang, Z.: Effects of Frozen Soil on Snowmelt Runoff and Soil Water Storage at a
581 Continental Scale, *J. Hydrometeorol.*, 7, 937–952, doi:10.1175/JHM538.1, 2006.

582 Oberbauer, S., Tweedie, C., Welker, J. M., Fahnestock, J. T., Henry, G. H. R., Webber, P. J., Hollister, R.
583 D., Walker, D. A., Kuchy, A., Elmore, E. and Starr, G.: Tundra CO₂ fluxes in response to experimental
584 warming across latitudinal and moisture gradients, *Ecol. ...*, 77(2), 221–238 [online] Available from:
585 <http://www.esajournals.org/doi/abs/10.1890/06-0649> (Accessed 10 July 2014), 2007.

586 Olefeldt, D., Goswami, S., Grosse, G., Hayes, D., Hugelius, G., Kuhry, P., McGuire, A. D., Romanovsky,
587 V. E., Sannel, A. B. K., Schuur, E. A. G. and Turetsky, M. R.: Circumpolar distribution and carbon
588 storage of thermokarst landscapes, *Nat. Commun.*, 7, 1–11, doi:10.1038/ncomms13043, 2016.

589 Oleson, K., Lawrence, D., Bonan, G., Drewniak, B., Huang, M., Koven, C., Levis, S., Li, F., Riley, W.,
590 Subin, Z., Swenson, S., Thornton, P., Bozbiyik, A., Fisher, R., Heald, C., Kluzek, E., Lamarque, J.-F.,
591 Lawrence, P., Leung, L., Lipscomb, W., Muszala, S., Ricciuto, D., Sacks, W., Sun, Y., Tang, J. and Yang,
592 Z.-L.: Technical description of version 4.5 of the Community Land Model (CLM), Boulder, Colorado.
593 [online] Available from: <http://opensky.library.ucar.edu/collections/TECH-NOTE-000-000-000-870>,
594 2013.

595 Ottlé, C., Lescure, J., Maignan, F., Poulter, B., Wang, T. and Delbart, N.: Use of various remote sensing
596 land cover products for plant functional type mapping over Siberia., *Earth Syst. Sci. Data*, 5(2), 331,
597 2013.

598 Peng, S., Ciais, P., Krinner, G., Wang, T., Gouttevin, I., McGuire, A. D., Lawrence, D., Burke, E., Chen,
599 X., Delire, C., Koven, C., MacDougall, A., Rinke, A., Saito, K., Zhang, W., Alkama, R., Bohn, T. J.,
600 Decharme, B., Hajima, T., Ji, D., Lettenmaier, D. P., Miller, P. A., Moore, J. C., Smith, B. and Sueyoshi,
601 T.: Simulated high-latitude soil thermal dynamics during the past four decades, *Cryosph. Discuss.*, 9(2),
602 2301–2337, doi:10.5194/tcd-9-2301-2015, 2015.

603 Rawlins, M. a., Steele, M., Holland, M. M., Adam, J. C., Cherry, J. E., Francis, J. a., Groisman, P. Y.,
604 Hinzman, L. D., Huntington, T. G., Kane, D. L., Kimball, J. S., Kwok, R., Lammers, R. B., Lee, C. M.,
605 Lettenmaier, D. P., McDonald, K. C., Podest, E., Pundsack, J. W., Rudels, B., Serreze, M. C.,
606 Shiklomanov, A., Skagseth, Ø., Troy, T. J., Vörösmarty, C. J., Wenshanan, M., Wood, E. F., Woodgate,
607 R., Yang, D., Zhang, K. and Zhang, T.: Analysis of the Arctic System for Freshwater Cycle
608 Intensification: Observations and Expectations, *J. Clim.*, 23(21), 5715–5737,
609 doi:10.1175/2010JCLI3421.1, 2010.

610 Ringeval, B., Decharme, B., Piao, S. L., Ciais, P., Papa, F., De Noblet-Ducoudré, N., Prigent, C.,
611 Friedlingstein, P., Gouttevin, I., Koven, C. and Ducharne, a.: Modelling sub-grid wetland in the
612 ORCHIDEE global land surface model: Evaluation against river discharges and remotely sensed data,
613 *Geosci. Model Dev.*, 5, 941–962, doi:10.5194/gmd-5-941-2012, 2012.

614 Roach, J., Griffith, B., Verbyla, D. and Jones, J.: Mechanisms influencing changes in lake area in Alaskan

615 boreal forest, *Glob. Chang. Biol.*, 17(8), 2567–2583, doi:10.1111/j.1365-2486.2011.02446.x, 2011.

616 De Rosnay, P. and Polcher, J.: Modelling root water uptake in a complex land surface scheme coupled to
617 a GCM, *Hydrol. Earth Syst. Sci.*, 2(2/3), 239–255, doi:10.5194/hess-2-239-1998, 1998.

618 De Rosnay, P., Bruen, M. and Polcher, J.: Sensitivity of surface fluxes to the number of layers in the soil
619 model used in GCMs, *Geophys. Res. Lett.*, 27(20), 3329–3332, doi:10.1029/2000GL011574, 2000.

620 Schädel, C., Bader, M. K.-F., Schuur, E. A. G., Biasi, C., Bracho, R., Čapek, P., De Baets, S., Diáková,
621 K., Ernakovich, J., Estop-Aragones, C., Graham, D. E., Hartley, I. P., Iversen, C. M., Kane, E.,
622 Knoblauch, C., Lupascu, M., Martikainen, P. J., Natali, S. M., Norby, R. J., O'Donnell, J. A., Chowdhury,
623 T. R., Šantrůčková, H., Shaver, G., Sloan, V. L., Treat, C. C., Turetsky, M. R., Waldrop, M. P. and
624 Wickland, K. P.: Potential carbon emissions dominated by carbon dioxide from thawed permafrost soils,
625 *Nat. Clim. Chang.*, 6(10), 950–953, doi:10.1038/nclimate3054, 2016.

626 Schaefer, K., Zhang, T., Bruhwiler, L. and Barrett, A. P.: Amount and timing of permafrost carbon
627 release in response to climate warming, *Tellus, Ser. B Chem. Phys. Meteorol.*, 63(2), 165–180,
628 doi:10.1111/j.1600-0889.2011.00527.x, 2011.

629 Sheffield, J., Goteti, G. and Wood, E. F.: Development of a 50-year high-resolution global dataset of
630 meteorological forcings for land surface modeling, *J. Clim.*, 19(13), 3088–3111, doi:10.1175/JCLI3790.1,
631 2006.

632 Slater, A. G. and Lawrence, D. M.: Diagnosing present and future permafrost from climate models, *J.*
633 *Clim.*, 26(15), 5608–5623, doi:10.1175/JCLI-D-12-00341.1, 2013.

634 Slater, A. G., Bohn, T. J., McCreight, J. L., Serreze, M. C. and Lettenmaier, D. P.: A multimodel
635 simulation of pan-Arctic hydrology, *J. Geophys. Res. Biogeosciences*, 112(4), 1–17,
636 doi:10.1029/2006JG000303, 2007.

637 Smith, L. C., Sheng, Y., MacDonald, G. M. and Hinzman, L. D.: Disappearing Arctic lakes., *Science*,
638 308(5727), 1429, doi:10.1126/science.1108142, 2005.

639 Streletskiy, D. A., Shiklomanov, N. I., Nelson, F. E. and Klene, A. E.: 13 Years of Observations at
640 Alaskan CALM Sites : Long-term Active Layer and Ground Surface Temperature Trends, in Ninth
641 International Conference on Permafrost, edited by D. L. Kane and K. M. Hinkel, pp. 1727–1732,
642 University of Alaska at Fairbanks, Fairbanks, AK., 2008.

643 Swenson, S. C., Lawrence, D. M. and Lee, H.: Improved simulation of the terrestrial hydrological cycle in
644 permafrost regions by the Community Land Model, *J. Adv. Model. Earth Syst.*, 4(8), 1–15,
645 doi:10.1029/2012MS000165, 2012.

646 Thornthwaite, C. and Mather, J. R.: Instructions and tables for computing potential evapotranspiration
647 and the water balance: Centeron, N.J., Laboratory of Climatology., *Publ. Climatol.*, 10(3), 185–311, 1957.

648 Throckmorton, H. M., Heikoop, J. M., Newman, B. D., Altmann, G. L., Conrad, M. S., Muss, J. D.,
649 Perkins, G. B., Smith, L. J., Torn, M. S., Wullschleger, S. D. and Wilson, C. J.: Pathways and
650 transformations of dissolved methane and dissolved inorganic carbon in Arctic tundra watersheds:
651 Evidence from analysis of stable isotopes, *Global Biogeochem. Cycles*, 29, 1893–1910,
652 doi:10.1002/2014GB005044.Received, 2015.

653 Walvoord, M. A. and Kurylyk, B. L.: Hydrologic Impacts of Thawing Permafrost—A Review, *Vadose*
654 *Zo. J.*, 15(6), 0, doi:10.2136/vzj2016.01.0010, 2016.

655 Wang, W., Rinke, A., Moore, J. C., Ji, D., Cui, X., Peng, S., Lawrence, D. M., McGuire, A. D., Burke, E.
656 J., Chen, X., Decharme, B., Koven, C., MacDougall, A., Saito, K., Zhang, W., Alkama, R., Bohn, T. J.,
657 Ciais, P., Delire, C., Gouttevin, I., Hajima, T., Krinner, G., Lettenmaier, D. P., Miller, P. A., Smith, B.,
658 Sueyoshi, T. and Sherstiukov, A. B.: Evaluation of air-soil temperature relationships simulated by land
659 surface models during winter across the permafrost region, *Cryosphere*, 10(4), 1721–1737,
660 doi:10.5194/tc-10-1721-2016, 2016.

661 Wania, R., Ross, I. and Prentice, I. C.: Integrating peatlands and permafrost into a dynamic global
662 vegetation model : 1 . Evaluation and sensitivity of physical land surface processes, , 23, 1–19,
663 doi:10.1029/2008GB003412, 2009a.

664 Wania, R., Ross, I. and Prentice, I. C.: Integrating peatlands and permafrost into a dynamic global
665 vegetation model : 2 . Evaluation and sensitivity of vegetation and carbon cycle processes, , 23, 1–15,

666 doi:10.1029/2008GB003413, 2009b.
667 Willmott, C. J. and Matsuura, K.: Terrestrial air temperature and precipitation: Monthly and annual time
668 series (1950–1999) Version 1.02., 2001.
669
670